

Showcasing research from Professor Knölker's laboratory, Faculty of Chemistry, Technical University of Dresden, Dresden, Germany.

μ -Oxo-bis[(octacosafuoro-*meso*-tetraphenylporphyrinato) iron(III)] – synthesis, crystal structure, and catalytic activity in oxidation reactions

The perfluorinated μ -oxo-bis[(*meso*-tetraphenylporphyrinato) iron(III)] complex represents a useful catalyst for highly efficient C–H bond activations. Applications include the regioselective oxidative couplings of diarylamines to 2,2'-bis(arylamino)-1,1'-biaryls and of carbazoles to 1,1'-, 3,3'-, and 4,4'-bicarbazoles using air as terminal oxidant. The latter coupling has been exploited for the first total synthesis of the bicarbazole alkaloid integerrine B. An atroposelective synthesis of biaryl compounds in up to 96% ee is feasible by asymmetric oxidative biaryl coupling in the presence of a chiral biaryl phosphoric acid. The iron-catalyzed Wacker-type oxidation of olefins provides a simple route to the corresponding ketones and gives excellent results even for internal olefins, previously considered as difficult substrates.

As featured in:



See Hans-Joachim Knölker *et al.*, *Chem. Sci.*, 2023, **14**, 257.

Cite this: *Chem. Sci.*, 2023, 14, 257

All publication charges for this article have been paid for by the Royal Society of Chemistry

μ -Oxo-bis[(octacosafuoro-meso-tetraphenylporphyrinato)iron(III)] – synthesis, crystal structure, and catalytic activity in oxidation reactions†

Tristan Schuh,  Olga Kataeva  and Hans-Joachim Knölker *

We describe the synthesis and X-ray crystal structure of μ -oxo-bis[(octacosafuoro-meso-tetraphenylporphyrinato)iron(III)] [(FeTPPF₂₈)₂O]. This novel iron complex is an efficient catalyst for oxidative biaryl coupling reactions of diarylamines and carbazoles. The asymmetric oxidative coupling in the presence of an axially chiral biaryl phosphoric acid as co-catalyst provides the 2,2'-bis(arylamino)-1,1'-biaryl in 96% ee. The Wacker-type oxidation of alkenes to the corresponding ketones with (FeTPPF₂₈)₂O as catalyst in the presence of phenylsilane proceeds at room temperature with air as the terminal oxidant. For internal and aliphatic alkenes increased ketone/alcohol product ratios were obtained.

Received 3rd November 2022
Accepted 6th December 2022

DOI: 10.1039/d2sc06083c

rsc.li/chemical-science

Introduction

Limited resources and environmental issues have promoted the development of sustainable chemistry. In organometallic catalysis the classical noble metals like palladium and iridium, which are expensive and toxic, are being replaced by first row transition metals. Among those, iron is the prime candidate for environmentally benign organometallic catalysis because of its high abundance and low toxicity.^{1,2} In nature, porphyrin-iron complexes are essential biocatalysts with cytochrome P450 enzymes as the most important class. These oxidoreductases occur in nearly all organisms.³ Moreover, they also catalyze uncommon transformations like rearrangements, cyclizations, and intramolecular C–C and C–heteroatom coupling reactions.^{4–10} These reactions generally proceed either *via* a hydrogen atom transfer (HAT) or single-electron transfer (SET) process.^{11,12} Therefore, the design of novel electron-deficient porphyrin-iron complexes could open up the way to unprecedented biomimetic reactions for organic synthesis. In this respect, the properties of μ -oxo-bridged binuclear porphyrinoid complexes have recently attracted a lot of attention.^{13,14}

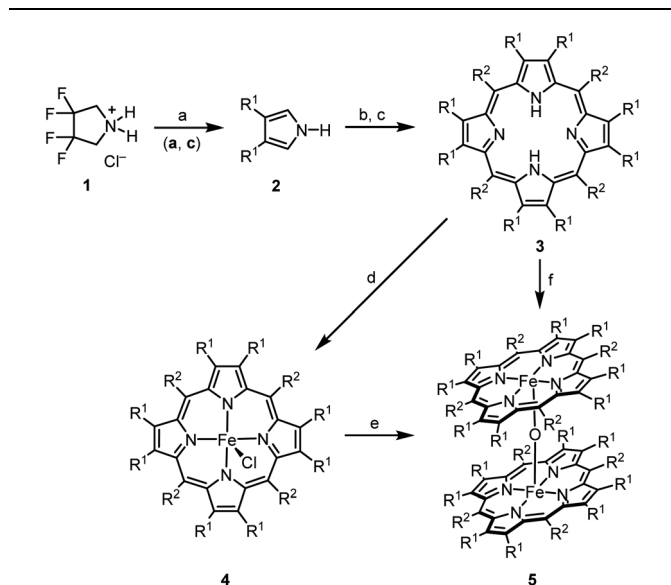
Results and discussion

In the present study,† we describe the synthesis, structural characterization, and applications in catalysis of the strongly electron-deficient complex μ -oxo-bis[(octacosafuoro-meso-tetraphenylporphyrinato)iron(III)] [(FeTPPF₂₈)₂O] (**5c**) (Table 1). We focused our efforts on the fluorinated porphyrin ligands, since in addition to the electron-withdrawing effect of the fluorine atoms they improve considerably the solubility of the complexes.^{15,16}

Homogeneous catalysis sometimes suffers from low solubility. However, moderately fluorinated organometallic complexes generally allow a broader spectrum of solvents that can be used. The first syntheses of β -octafluoro-substituted meso-tetraphenylporphyrins and their zinc complexes were reported independently by two different groups in 1997.^{17,18} The direct introduction of fluorine substituents at the porphyrin ring is not possible and thus β -octafluoro-meso-tetraphenylporphyrins (**3a** and **3c**) are synthesized by condensation of 3,4-difluoropyrrole (**2a**) with the corresponding benzaldehydes. The β -octafluorinated porphyrins **3a** and **3c** are accessible from 3,3,4,4-tetrafluoropyrrolidinium chloride (**1**) *via* a three-step sequence reported by DiMaggio *et al.*^{18,19} According to ¹H and ¹⁹F NMR analysis (see SI), the elimination of hydrogen fluoride proceeds nearly quantitatively. However, DiMaggio *et al.* isolated 3,4-difluoropyrrole (**2a**) in only 53% yield due to the extremely high volatility of this compound.¹⁹ We found that the overall yield of the porphyrins **3a** and **3c** is considerably improved by avoiding the isolation of **2a** and submitting the crude product directly to the cyclocondensation step. The formation of the fluorinated tetraphenylporphyrin-iron complexes **4a–4c** from the corresponding porphyrins using the classical conditions

Fakultät Chemie, Technische Universität Dresden, Bergstrasse 66, 01069 Dresden, Germany. E-mail: hans-joachim.knoelker@tu-dresden.de; Web: <https://tu-dresden.de/mn/chemie/oc/oc2>; Fax: +49 351-463-37030

† Electronic supplementary information (ESI) available: Synthetic procedures and full characterization for all compounds, spectroscopic data, copies of the ¹H, ¹³C, and ¹⁹F spectra, crystallographic data. CCDC 2209872 and 2209883. For ESI and crystallographic data in CIF or other electronic format see DOI: <https://doi.org/10.1039/d2sc06083c>

Table 1 Synthesis of the fluorinated μ -oxo-porphyrin-iron(III) complexes **5^a**

	R ¹	R ²	3	4, Yield [%]	5, Yield [%]
a	F	C ₆ H ₅	H ₂ TPPF ₈	FeTPPF ₈ Cl, 59	—
b	H	C ₆ F ₅	H ₂ TPPF ₂₀	FeTPPF ₂₀ Cl, 96	(FeTPPF ₂₀) ₂ O, 98
c	F	C ₆ F ₅	H ₂ TPPF ₂₈	FeTPPF ₂₈ Cl, 92	(FeTPPF ₂₈) ₂ O, >99

^a Reaction conditions: (a) **1** (1.0 equiv.), KO^t-Bu (4.0 equiv.), DMSO, Ar, rt, 0.5 h; (b) **2** (1.0 equiv.), R²CHO (1.1 equiv.), BF₃·OEt₂ (4.0 equiv.), CH₂Cl₂, Ar, rt; (c) DDQ (1.0 equiv.), pyridine (8.0 equiv.), Ar, rt; (d) FeCl₂ (20 equiv.), MeCN, air, 120 °C, 4 h, sealed tube; (e) activated alumina, CH₂Cl₂/MeOH (95 : 5), air, rt; (f) FeCl₂ (20 equiv.), MeCN, air, 120 °C, 4 h, sealed tube; followed by elution of the crude product over activated alumina, CH₂Cl₂/MeOH (95 : 5), air, rt (see ESI for details).

described by Adler (DMF at reflux)²⁰ led to a complex reaction mixture. This mixture is resulting from nucleophilic aromatic substitution at the fluorinated porphyrins by dimethylamine, formed by decarbonylation of the solvent. Adapting the conditions reported by Freire *et al.*, complexation of **3a–3c** was achieved by reaction with iron(II) chloride in acetonitrile at 120 °C.²¹

Several preparations of μ -oxo-porphyrinoid-iron complexes have been reported.^{13,14,22,23} The β -octafluoro-substituted μ -oxo-iron complex (FeTPPF₈)₂O (**5a**) could not be prepared due to the extremely low solubility of the corresponding chloro-iron complex **4a**. Complex **5b** was described previously.²⁴ Elution of the chloro complex **4c** over activated alumina (CH₂Cl₂/MeOH, 95 : 5) provided quantitatively the μ -oxo complex (FeTPPF₂₈)₂O (**5c**).

Deep red cubic crystals of complex **5c** suitable for X-ray crystallography were obtained by recrystallization from dichloromethane (Fig. 1).²⁵ The geometry of **5c** is similar to the previously reported structures of the μ -oxo-bis[(tetraphenylporphyrinato)iron(III)] complexes (FeTPPF₂₀)₂O (**5b**) and (FeTPP)₂O.^{24,26} Remarkable is the central, nearly linear Fe–O–Fe axis with a bond angle of 178.34(19)°,²⁵ which is more similar to the 178.4(5)° reported for the fluorinated complex (FeTPPF₂₀)₂O (**5b**)²⁴ rather than to the 174.5(1)° of the non-fluorinated complex (FeTPP)₂O.²⁶ In contrast, the structurally related

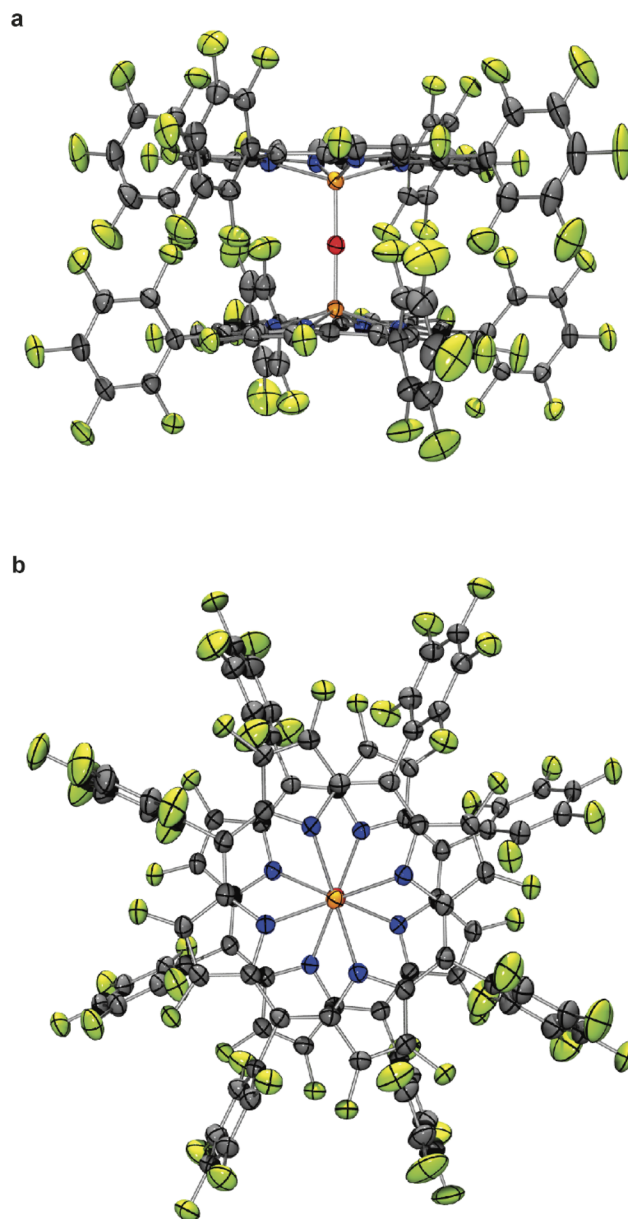


Fig. 1 Molecular structure of μ -oxo-bis[octacosafuoro-*meso*-tetraphenylporphyrinato]iron(III) (**5c**) in the crystal (thermal ellipsoids are shown at the 50% probability level); (a) side view; (b) view along the Fe–O–Fe axis. Bond length Fe–O 1.7816(6) Å; bond angle Fe–O–Fe 178.34(19)°.

μ -oxo-porphyrinoid-iron complexes μ -oxo-bis[(phthalocyaninato)iron(III)]^{13b} can adopt a tilted or nearly linear geometry and μ -oxo-bis[(octapropylporphyrinato)iron(III)]¹³ has a more bent Fe–O–Fe bond angle of 158.52(7)°^{13a,27} as compared to the aforementioned porphyrin-iron complexes. The Fe–O bond length of complex **5c** (1.7816(6) Å)²⁵ is slightly longer than in the related porphyrinoid-iron complexes (FeTPPF₂₀)₂O (**5b**) (1.775(1) Å),²⁴ (FeTPP)₂O (1.763(1) Å),²⁶ and μ -oxo-bis[(octapropylporphyrinato)iron(III)] (1.7601(12), 1.7501(12) Å).^{13a}

Leroy *et al.* investigated the catalytic activity of the porphyrinato-iron(III) chloride complexes **4a** and **4c** for epoxidation and



hydroxylation reactions.^{28a} Very recently, Fujii *et al.* transformed **4b** and **4c** into the corresponding hypochlorite complexes and studied their catalytic reactivity in epoxidation and chlorination reactions.^{28b}

Previously, we described iron-catalyzed oxidative C–C and C–heteroatom coupling reactions using hexadecafluorophthalocyanine–iron(II) (FePcF₁₆) as well as the corresponding μ -oxo-iron(III) complex ([FePcF₁₆]₂O) as catalysts and air as terminal oxidant.²⁹ We have now studied in detail the catalytic activity of the fluorinated porphyrin–iron(III) complexes **4a–4c**, **5b**, and **5c** in oxidative coupling reactions. We postulated that the strong electron-withdrawing effect of the fluorine atom should increase the catalytic activity of (FeTPPF₂₈)₂O (**5c**) as compared to the unsubstituted FeTPP system in analogy to our observations with the perfluorinated phthalocyanine–iron complexes. The oxidative C–C homocoupling of *N*-phenyl-2-naphthylamine (**6**) was selected as model system. Using the previously reported catalyst FePcF₁₆ and methanesulfonic acid (MsOH) as additive, the biaryl compound **7** was isolated in 62% yield along with 11% of the carbazole **8** (Table 2, entry 1; Fig. 2).³⁰ Initial attempts with the unsubstituted *meso*-tetraphenylporphyrin–iron complex FeTPPCL and the corresponding β -octafluorinated complex **4a** in the presence of methanesulfonic acid as additive gave no turnover (Table 2, entries 2 and 3). The perfluorinated complex FeTPPF₂₈Cl (**4c**) gave only traces of the product **7** (entry

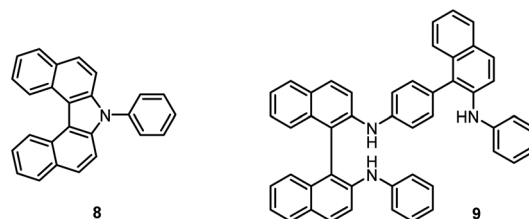
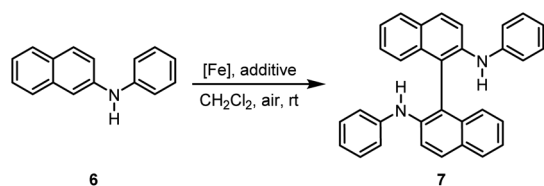


Fig. 2 Isolated by-products: carbazole **8** and the twofold coupling product **9**.

4). In conclusion, none of the chloro complexes **4a–4c** showed significant catalytic activity in the C–C coupling of **6**.

The μ -oxo-iron complexes are assumed to be intermediates in the catalytic cycle of oxidations with porphyrin and phthalocyanine–iron complexes.^{13,14,29,31} Thus, we tested the μ -oxo-iron complex (FeTPPF₂₈)₂O (**5c**) as catalyst under the same conditions used above for the complexes **4a–4c** and obtained the biaryl **7** in 6% yield (entry 5). Performing the reaction under an atmosphere of pure oxygen improved the yield only slightly (entry 6). Variation of the additive improved the yield significantly and revealed that strong Brønsted acids (TFA and TfOH, entries 8 and 9) and the Lewis acids tris(pentafluorophenyl)borane (entry 10) and boron trifluoride diethyl etherate (entry 11) gave the best results. Control experiments confirmed that both the iron catalyst (entry 12) and the Lewis acid (entry 13) are required for the reaction to proceed. The iron-catalyzed oxidative coupling of **6** was generally performed using non-dried solvents under an ambient atmosphere. Finally, we have demonstrated that water-free conditions with dried air and anhydrous solvents led to a further slight increase of the yield of **7** and a decrease of the reaction time (entry 14).

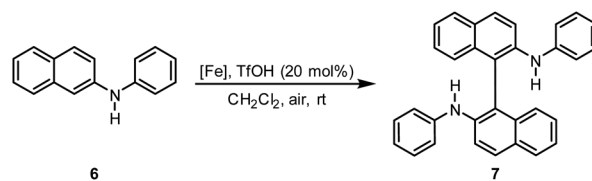
Table 2 Optimization of the reaction conditions for the tetraphenylporphyrin–iron-catalyzed oxidative C–C coupling of *N*-phenyl-2-naphthylamine (**6**)^a



Entry	[Fe] (mol%)	Additive (mol%)	Time [h]	Yield 7 [%]
1 ³⁰	FePcF ₁₆ (3.0)	MsOH (10)	0.5	62 ^b
2	FeTPPCL (3.0)	MsOH (20)	24	0
3	FeTPPF ₈ Cl (4a) (3.0)	MsOH (20)	24	0
4	FeTPPF ₂₈ Cl (4c) (3.0)	MsOH (20)	73	Traces
5	(FeTPPF ₂₈) ₂ O (5c) (1.5)	MsOH (20)	49	6
6 ^c	(FeTPPF ₂₈) ₂ O (5c) (1.5)	MsOH (20)	62	12
7	(FeTPPF ₂₈) ₂ O (5c) (1.5)	AcOH (20)	60	5
8	(FeTPPF ₂₈) ₂ O (5c) (1.5)	TFA (20)	40	60 ^d
9	(FeTPPF ₂₈) ₂ O (5c) (1.5)	TfOH (20)	48	78 ^e
10	(FeTPPF ₂₈) ₂ O (5c) (1.5)	B(C ₆ F ₅) ₃ (20)	18	80
11	(FeTPPF ₂₈) ₂ O (5c) (1.5)	BF ₃ ·OEt ₂ (20)	14	76 ^f
12	—	BF ₃ ·OEt ₂ (20)	24	0
13	(FeTPPF ₂₈) ₂ O (5c) (1.5)	—	24	0
14 ^g	(FeTPPF ₂₈) ₂ O (5c) (1.5)	BF ₃ ·OEt ₂ (20)	5	84

^a Reaction conditions: **6** (0.1 mmol), additive, CH₂Cl₂ (2 mL), air, rt. ^b **8**: 11% yield, reisolated **6**: 7%. ^c Molecular oxygen (1 atm). ^d **8**: 3% yield, reisolated **6**: 37%. ^e **9**: 9% yield. ^f **9**: 7% yield. ^g Water-free conditions, 3 Å MS, dried compressed air. Pc = phthalocyanine, TPP = tetraphenylporphyrin.

Table 3 Variation of the tetraphenylporphyrin–iron(III) complexes in the oxidative C–C coupling of *N*-phenyl-2-naphthylamine (**6**)^a



Entry	[Fe] (mol%)	Yield 7 [%]	Reisolated 6 [%]
1	FeTPPCL (3.0)	0	99
2	FeTPPF ₈ Cl (4a) (3.0)	6	93
3	FeTPPF ₂₀ Cl (4b) (3.0)	5	89
4	FeTPPF ₂₈ Cl (4c) (3.0)	7	90
5	(FeTPPF ₂₀) ₂ O (5b) (1.5)	57	21 ^b
6	(FeTPPF ₂₈) ₂ O (5c) (1.5)	78	0 ^c
7 ^d	FeTPPF ₂₈ Cl (4c) (3.0)	89	0 ^e

^a Reaction conditions: **6** (0.1 mmol), TfOH (20 mol%), CH₂Cl₂ (2 mL), air, rt, 48 h. ^b **8**: 11% yield. ^c **9**: 9% yield. ^d AgOTf (3 mol%), 4 h. ^e **9**: 8% yield.



Under the optimized reaction conditions identified above (Table 2, entry 9), the effect of the fluorine substitution and of the axial ligand at the iron atom was investigated using the porphyrin complexes **FeTPPFCl**, **4a–4c**, **5b**, and **5c** as catalysts (Table 3). Two general trends have been observed. The complex **FeTPPFCl** had no catalytic activity at all and the complexes **4a–4c** exhibited a very low catalytic activity providing **7** in yields below 10% (Table 3, entries 1–4). However, the μ -oxo-iron complexes (**FeTPPF₂₀**)₂O (**5b**) and (**FeTPPF₂₈**)₂O (**5c**) led to much higher turnover numbers and provided **7** in yields of 57 and 78%, respectively (entries 5 and 6). We concluded that the significant difference in catalytic activity is caused by the different axial ligand. Thus using the chloro-iron complex **4c**, we added 3 mol% of silver triflate to the reaction mixture in order to generate *in situ* **FeTPPF₂₈OTf**, which led to much shorter reaction times (4 h instead of 48 h) and afforded the biaryl compound **7** in 89% yield (entry 7).

Based on our experimental findings, we postulate the following mechanism for the (**FeTPPF₂₈**)₂O-catalyzed oxidative coupling considering the strong influence of the additive (Scheme 1). The reaction is believed to be initiated by an SET oxidation followed by coupling and proton loss.³²

The key step is an SET from the substrate to the iron(III) complex, as previously observed by Baciocchi *et al.* for the oxidation of *N,N*-dimethylanilines with **FeTPPF₂₀Cl** (**4b**).^{12b} The SET process is much more efficient with strongly electron-deficient iron(III) complexes. Chen *et al.* found that *in situ* exchange of the axial ligand from chloride to triflate enhances the reactivity of porphyrin-iron(III) complexes for oxidation reactions significantly since triflate is a weaker donor than chloride.³³ In order to rationalize our experimental findings

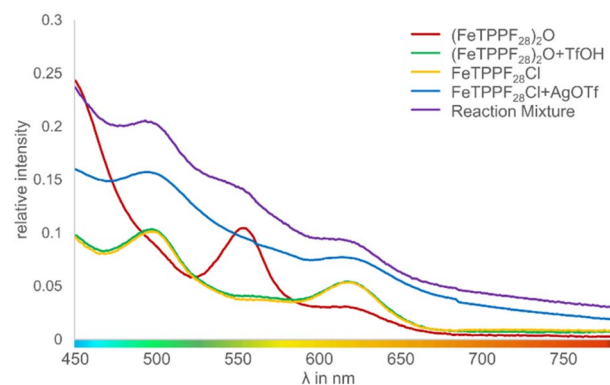
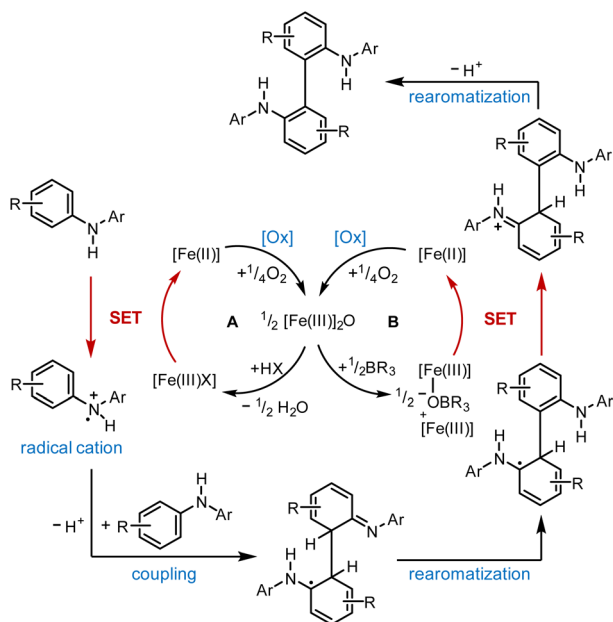


Fig. 3 UV-vis spectra of different iron species involved in the oxidative coupling reaction (intensity of the Soret peak normalized to 1; Fig. S1†).

described above, we followed the iron-catalyzed oxidative coupling by UV-vis experiments (Fig. 3 and S1†).

We observed that the μ -oxo complex (**FeTPPF₂₈**)₂O (**5c**) is rapidly hydrolyzed by strong Brønsted acids. After addition of TfOH to a solution of **5c**, the characteristic peak at 553 nm disappeared whereas two peaks at 497 and 618 nm emerged, which are assigned to the complex **FeTPPF₂₈OTf**. Alternatively, the latter complex can be generated *in situ* by reaction of **FeTPPF₂₈Cl** (**4c**) with silver trifluoromethanesulfonate. The UV-vis spectrum of the reaction mixture with **5c** as catalyst and TfOH as additive showed after 1 hour all three peaks, indicating that both porphyrin-iron(III) triflate and the μ -oxo complex **5c** are present. Thus, using the μ -oxo complex (**FeTPPF₂₈**)₂O (**5c**) in combination with a strong acid (TfOH) as catalyst generates a catalytic system more reactive than **FeTPPF₂₈Cl** (**4c**) (Table 3, entries 4 *versus* 6). Additional support derives from the increase in catalytic activity observed by exchange of the chloro against the triflate ligand (Table 3, entries 4 and 7).

We have studied the catalytic activity of (**FeTPPF₂₈**)₂O (**5c**) for the oxidative coupling of a selection of diarylamines **10a–10c** (Table 4). The variation of the additive showed that the Lewis acid **BF₃·OEt₂** was more efficient than the previously used



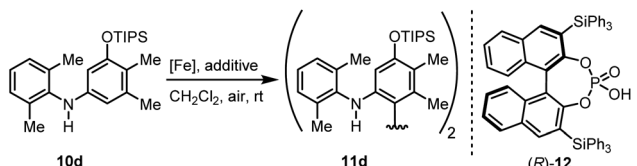
Scheme 1 Proposed mechanism for the (**FeTPPF₂₈**)₂O-catalyzed biaryl coupling. Cycle A: Brønsted acid co-catalyst; cycle B: Lewis acid co-catalyst. X = OTf; [Fe(III)]₂O = **5c**.

Table 4 (**FeTPPF₂₈**)₂O-catalyzed oxidative C–C coupling of the diarylamines **10a–10c**^a

Entry	Diarylamine	R ¹	R ²	t [h]	Yield 11 [%]
1	10a	H	H	24	70 ^b
2	10b	H	OPiv	20	75
3	10c	OPiv	H	22	78

^a Reaction conditions: **10** (0.1 mmol), (**FeTPPF₂₈**)₂O (**5c**) (1.5 mol%), **BF₃·OEt₂** (20 mol%), **CH₂Cl₂** (2 mL), air, rt. ^b Reisolated **10a**: 8%.

Table 5 Asymmetric (FeTPPF₂₈)₂O-catalyzed oxidative C–C coupling^a

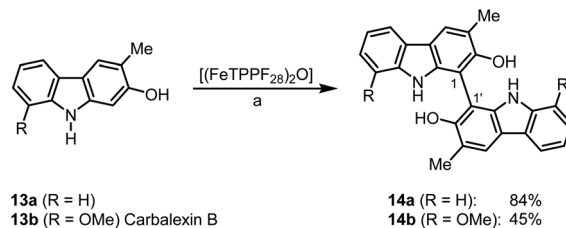
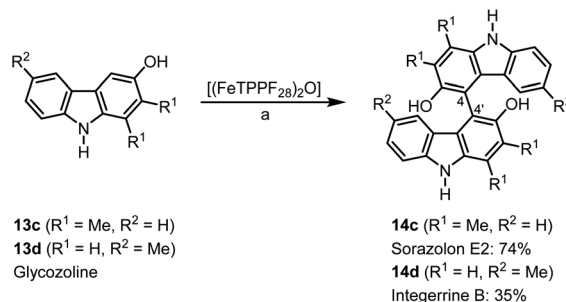
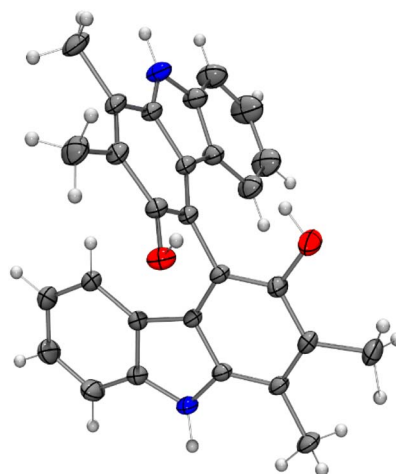
					
Entry	[Fe] (mol%)	Additive (mol%)	t [h]	Yield 11d [%]	ee [%] ^b
1 ³⁰	FePcF ₁₆ (3.0)	(<i>R</i>)- 12 (10)	24	71 ^c	90
2	(FeTPPF ₂₈) ₂ O (1.5)	BF ₃ ·OEt ₂ (20)	23	71	0
3	(FeTPPF ₂₈) ₂ O (1.5)	(<i>R</i>)- 12 (20)	72	64	96

^a Reaction conditions: **10d** (0.1 mmol), [Fe], additive, CH₂Cl₂ (2 mL), air, rt. ^b Determined by chiral HPLC (see: Fig. S2 and S3†). ^c Reisolated **10d**: 18%.

Brønsted acids (Table S1†). Using these modified conditions, the coupling of **10a–10c** proceeded more slowly but gave improved yields compared to our previous results using FePcF₁₆ as catalyst.^{29a}

We then explored the possibility to achieve an asymmetric catalytic oxidative coupling of **10d** to the atropisomeric biaryl compound **11d** using (FeTPPF₂₈)₂O (**5c**) as catalyst (Table 5). 1,1'-Biaryl-2,2'-phosphoric acids have been established as efficient chiral catalysts for asymmetric catalysis by Akiyama, Terada, and List.³⁴ Recently, we have shown that oxidation of **10d** with FePcF₁₆ as catalyst in the presence of 10 mol% of the chiral phosphoric acid (*R*)-**12** as co-catalyst afforded **11d** in 71% yield and 90% ee (Table 5, entry 1).³⁰ The chiral phosphate counter-ion was believed to direct the asymmetric coupling of the radical cation generated from **10d** by an initial single-electron transfer. Using **5c** as catalyst in the presence of 20 mol% of (*R*)-**12** led to the biaryl compound **11d** in 96% ee (Table 5, entry 3).

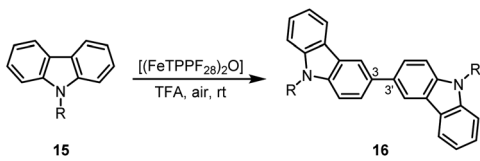
Bicarbazoles are an important class of biologically active natural products which can be prepared by C–H/C–H coupling reactions.^{35,36} Recently, we described the synthesis of various bicarbazole alkaloids by FePcF₁₆-catalyzed oxidative coupling.³⁷ Using (FeTPPF₂₈)₂O (**5c**) as catalyst for the iron-catalyzed oxidative homocoupling of carbazoles offers a broad structural variety of 1,1'-, 3,3'-, and 4,4'-linked bicarbazoles. The oxidative coupling of 2-hydroxy-3-methylcarbazole (**13a**)³⁸ and carbalexin B (**13b**)³⁹ using 1.5 mol% of (FeTPPF₂₈)₂O (**5c**) as catalyst in the presence of 20 mol% of BF₃·OEt₂ provided regioselectively the naturally occurring 1,1'-bicarbazole alkaloid bis-2-hydroxy-3-methylcarbazole (**14a**)⁴⁰ and biscarbalexin B (**14b**)³⁷ (Scheme 2). 4,4'-Bicarbazoles as natural products have been isolated only recently. Oxidative coupling of 3-hydroxy-1,2-dimethyl-9*H*-carbazole (**13c**)⁴¹ in the presence of (FeTPPF₂₈)₂O as catalyst provided sorazolon E2 (**14c**)⁴² (Scheme 3). The structure of **14c** was confirmed by an X-ray crystal structure determination (Fig. 4).⁴³ Analogously, the oxidative homocoupling of glycozoline (**13d**)⁴⁴ led to the first synthesis of integerrine B (**14d**).⁴⁵ The ¹H and ¹³C NMR data of synthetic integerrine

**Scheme 2** (FeTPPF₂₈)₂O-catalyzed synthesis of 1,1'-bicarbazoles. Reaction conditions: a) **13** (0.15 mmol), (FeTPPF₂₈)₂O (**5c**) (1.5 mol%), BF₃·OEt₂ (20 mol%), CH₂Cl₂ (5 mL), air, rt.**Scheme 3** (FeTPPF₂₈)₂O-catalyzed synthesis of 4,4'-bicarbazoles. Reaction conditions: a) **13** (0.15 mmol), (FeTPPF₂₈)₂O (**5c**) (1.5 mol%), BF₃·OEt₂ (20 mol%), CH₂Cl₂ (15 mL), air, rt.**Fig. 4** Molecular structure of sorazolon E2 (**14c**) in the crystal (thermal ellipsoids are shown at the 50% probability level).

B (**14d**) are in excellent agreement with those reported for the natural product (Table S2†).

Due to their physical properties, 3,3'-bicarbazoles represent promising candidates for hole-transporting materials in organic light-emitting diodes (OLEDs).⁴⁶ Previous procedures for the synthesis of 3,3'-bicarbazoles by oxidative homocoupling required stoichiometric amounts of iron(III) chloride,⁴⁷ DDQ,⁴⁸ or rhodium as noble metal catalyst.⁴⁹ Our method using oxygen as terminal oxidant in the presence of (FeTPPF₂₈)₂O (**5c**) as catalyst



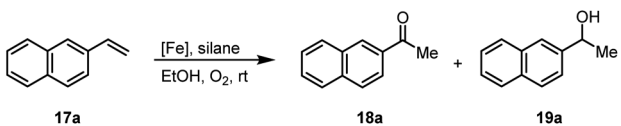
Table 6 (FeTPPF₂₈)₂O-catalyzed synthesis of 3,3'-bicarbazoles **16**^a


Entry	Carbazole	R	[Fe] (mol%)	t [h]	Yield 16 [%]
1	15a	Me	1.5	1.5	82
2	15b	Bn	1.5	18	71
3	15c	Ph	2.6	4.5	82

^a Reaction conditions: **15** (0.1 mmol), (FeTPPF₂₈)₂O (**5c**), TFA (2–4 mL), air, rt.

enables the first iron-catalyzed oxidative coupling of the carbazoles **15a–15c** to the 3,3'-bicarbazoles **16a–16c** (Table 6).

Another iron-catalyzed oxidation process recently investigated by our group is the Wacker-type oxidation of olefins to ketones.^{50–53} The oxidation of 2-vinylnaphthalene (**17a**) to 2-acetylnaphthalene (**18a**) served as a model system in order to test different phthalocyanine- and porphyrin-iron complexes under an atmosphere of pure oxygen (Table 7). Our previous results showed a much higher catalytic activity of the fluorinated phthalocyanine- and porphyrin-iron complexes as

Table 7 Porphyrinoid-iron complex-catalyzed Wacker-type oxidation of 2-vinylnaphthalene (**17a**)^a


Entry	[Fe] (mol%)	Silane	t [h]	Yield 18a [%]	Yield 19a [%]
1 ⁵⁰	FePc (5.0)	Et ₃ SiH ^b	23	17	8
2 ⁵¹	FePcF ₁₆ (5.0)	Et ₃ SiH	6	82	12
3 ⁵¹	FePcF ₁₆ (5.0)	Ph ₃ SiH	2.5	85	12
4 ⁵¹	FePcF ₁₆ (5.0)	PhSiH ₃	4	48	13
5 ⁵¹	(FePcF ₁₆) ₂ O (2.5)	Et ₃ SiH	10	84	13
6 ⁵¹	(FePcF ₁₆) ₂ O (2.5)	Ph ₃ SiH	4	85	12
7 ⁵⁰	FeTPPcI (5.0)	Et ₃ SiH	6	2	Traces
8 ⁵⁰	FeTPPF ₂₀ Cl (4b) (5.0)	Et ₃ SiH	6	22	4
9	FeTPPF ₂₀ Cl (4b) (5.0)	PhSiH ₃	24	74	Traces
10	(FeTPPF ₂₀) ₂ O (5b) (2.5)	Et ₃ SiH	24	0	0
11	(FeTPPF ₂₀) ₂ O (5b) (2.5)	PhSiH ₃	24	78	Traces
12	FeTPPF ₂₈ Cl (4c) (5.0)	Et ₃ SiH	24	0	0
13	FeTPPF ₂₈ Cl (4c) (5.0)	Ph ₃ SiH	24	0	0
14	FeTPPF ₂₈ Cl (4c) (5.0)	PhSiH ₃	24	76	9
15	(FeTPPF ₂₈) ₂ O (5c) (2.5)	Et ₃ SiH	24	0	0
16	(FeTPPF ₂₈) ₂ O (5c) (2.5)	Ph ₃ SiH	24	0	0
17	(FeTPPF ₂₈) ₂ O (5c) (2.5)	PhSiH ₃	24	78	10
18 ^c	(FeTPPF ₂₈) ₂ O (5c) (2.5)	PhSiH ₃	40	87	Traces

^a Reaction conditions: **17a** (0.2 mmol), silane (2.0 equiv), EtOH (5 mL), O₂ (1 atm), rt. ^b Et₃SiH (6.0 equiv.). ^c Air instead of pure O₂.

compared to their unsubstituted analogs (Table 7, entries 1–8).^{50,51} Moreover, the importance to use the appropriate silane reducing agent in combination with the corresponding iron catalyst was emphasized.^{50–53} The present results confirm this strong influence of the silane when using the iron complexes FeTPPF₂₀Cl (**4b**) and (FeTPPF₂₀)₂O (**5b**) as catalysts for the Wacker-type reaction (Table 7, entries 8–11). Based on these previous results, we expected a high catalytic activity for the iron complexes **4c** and **5c** with the perfluorinated porphyrinato ligand octacosafuoro-*meso*-tetraphenylporphyrin. To our surprise, we had no turnover at all in the oxidation of the olefin **17a** using FeTPPF₂₈Cl (**4c**) as catalyst and either triethylsilane or triphenylsilane as reducing agent under otherwise identical reaction conditions (Table 7, entries 12 and 13). Phenylsilane was proven to be the best reducing agent for the iron-catalyzed Wacker-type reaction with tris(1,3-diketono)iron(III) complexes as catalysts.⁵³ Indeed, using complex **4c** as catalyst in combination with phenylsilane provided the ketone **18a** in 76% yield along with 9% of the corresponding alcohol **19a** (Table 7, entry 14). Basically the same results were obtained for the oxidation of **17a** to **18a** using the three reducing agents Et₃SiH, Ph₃SiH, and PhSiH₃ in combination with (FeTPPF₂₈)₂O (**5c**) as catalyst (Table 7, entries 15–17). These results provide further evidence for our mechanistic hypothesis with μ -oxo[diiron(III)] complexes as intermediates in the catalytic cycle of the Wacker-type oxidation which also applies to the present reaction using complex **5c** as catalyst.⁵¹ Finally, we tested air instead of an atmosphere of pure oxygen as re-oxidant for our iron complex (Table 7, entry 18). Although the reaction time was prolonged, we were delighted that the yield of the desired product **18a** increased to 87%, whereas only traces of the alcohol **19a** could be detected.

Using (FeTPPF₂₈)₂O (**5c**) as catalyst under the optimized reaction conditions, we have tested the Wacker-type oxidation for a range of different olefins **17a–17h** (Table 8). A special focus was on those olefins which gave poor results in our previous study with FePcF₁₆ or [FePcF₁₆]₂O as catalysts, the cyclic olefins **17e–17g** and the aliphatic olefin **17h**.^{50–52} For the simple styrene derivatives **17a–17d**, the oxidation with **5c** as catalyst proceeded smoothly affording the corresponding ketones **18a–18d** in yields as high or even slightly better compared to those obtained with FePcF₁₆ as catalyst,⁵⁰ albeit longer reaction times were required. The differences between the results with (FeTPPF₂₈)₂O (**5c**) and the perfluorophthalocyanine-iron complex as catalyst were most pronounced for the oxidation of the more challenging substrates (cyclic olefins and aliphatic olefins). The results with the substrates **17e–17h** show that the selectivity of the reaction is shifted significantly towards the ketone at the expense of the alcohol by-product. For example, the Wacker-type oxidation of the nitrochromene **17e** catalyzed by (FeTPPF₂₈)₂O (**5c**) afforded the chroman-4-one **18e** in 79% yield along with only 11% of the corresponding alcohol **19e** (previous result with FePcF₁₆ as catalyst under O₂: 62% of **18e** and 35% of **19e**).⁵² Compound **18e** represents a synthetic precursor for the pyrano[3,2-*a*]carbazole alkaloid euchrestifoline.^{52–54} Also for the (FeTPPF₂₈)₂O-catalyzed oxidation of the cyanochromene **17f** and the dihydronaphthalene **17g** to the ketones **18f** (93% yield)



Table 8 Substrate scope and selectivity of the (FeTPPF₂₈)₂O-catalyzed Wacker-type oxidation^a

$ \begin{array}{c} \text{R}^1\text{---}\text{CH}=\text{CH}\text{---}\text{R}^2 \\ \text{17} \end{array} \xrightarrow[\text{PhSiH}_3, \text{EtOH, air, rt}]{[(\text{FeTPPF}_{28})_2\text{O}]} \begin{array}{c} \text{R}^1\text{---}\text{C}(=\text{O})\text{---}\text{CH}_2\text{---}\text{R}^2 \\ \text{18} \end{array} + \begin{array}{c} \text{R}^1\text{---}\text{CH}(\text{OH})\text{---}\text{CH}_2\text{---}\text{R}^2 \\ \text{19} \end{array} $			
17	Time [h]	Yield 18 [%]	Yield 19 [%]
a	40	87	Traces
b	24	90	0
c	76	89	0
d	48	85	7
e	62	79	11
f	71	93	6
g	48	89	5
h	120	53	11

^a Reaction conditions: 17 (0.2 mmol), (FeTPPF₂₈)₂O (2.5 mol%), PhSiH₃ (2.0–5.0 equiv.), EtOH (3 mL), air (1 atm), rt; see SI for details.

and **18g** (89% yield), we observed a much higher selectivity in favor of the ketones (previous yields with FePcF₁₆ as catalyst under O₂: 65% for **18f** and 68% for **18g**).⁵⁰ Most strikingly, oxidation of the aliphatic alkene 1-octadecene (**17h**) using (FeTPPF₂₈)₂O (**5c**) as catalyst provided 2-octadecanone (**18h**) in 53% yield,⁵⁵ whereas the corresponding reaction with FePcF₁₆ required more of the catalyst (10 mol%), pure oxygen as reoxidant, and elevated temperature (78 °C) but still led preferentially to the alcohol **19h** (42% yield) along with **18h** (30% yield).⁵⁰ Thus, we have shown that the Wacker-type oxidation of olefins using the new catalyst (FeTPPF₂₈)₂O (**5c**) proceeds smoothly with ambient air as final oxidant. The present reaction gives higher selectivities in favor of the desired ketones as compared to the corresponding reaction with FePcF₁₆ as catalyst which needs pure oxygen as reoxidant to achieve the best turnover numbers.

Conclusions

We have described the synthesis of the novel perfluorinated porphyrin-iron complex μ -oxo-bis[(octacosafuoro-*meso*-tetraphenylporphyrinato)iron(III)] [(FeTPPF₂₈)₂O]. The high activity of this catalyst in oxidation reactions has been demonstrated for the biaryl coupling and the Wacker-type reaction. The

twofold aryl C–H bond activation was exploited for the oxidative coupling of diarylamines leading to 2,2'-bis(arylamino)-1,1'-biaryls. In the presence of an axially chiral biaryl phosphoric acid as co-catalyst this coupling proceeds in up to 96% *ee*. The (FeTPPF₂₈)₂O-catalyzed oxidative coupling of 2-hydroxy-, 9-alkyl/aryl-, and 3-hydroxycarbazoles affords regioselectively 1,1', 3,3'-, and 4,4'-bicarbazoles and has been applied to the synthesis of a variety of bicarbazole natural products including the first synthesis of integerrine B. The Wacker-type oxidation of alkenes, including internal and aliphatic alkenes, previously considered as difficult substrates, with (FeTPPF₂₈)₂O as catalyst in the presence of phenylsilane proceeds at room temperature with air as terminal oxidant and provides the corresponding ketones in high yields. The present findings are paving the way for the development of mild and selective oxidation reactions under biomimetic conditions resembling those of the enzymatic oxidative processes in nature dependent on cytochrome P450 heme proteins.

Data availability

The data supporting this article have been uploaded as part of the ESI.†

Author contributions

H.-J. K. secured the funding and directed the project. T. S. and H.-J. K. conceived the project and designed the molecules. T. S. carried out the chemical syntheses, the catalytic experiments, and the structure characterizations. O. K. performed the X-ray crystal structure determinations and analyzed the data. T. S. and H.-J. K. wrote, reviewed, and edited the manuscript.

Conflicts of interest

There are no conflicts to declare.

Acknowledgements

We thank the Deutsche Forschungsgemeinschaft (DFG) for the financial support of our project "Green and Sustainable Catalysts for Synthesis of Organic Building Blocks" (DFG grant KN 240/19-2). We also like to thank the Deutscher Akademischer Austauschdienst (DAAD) for support (57507438).

Notes and references

† Part 153 of "Transition Metals in Organic Synthesis"; for part 152, see: ref. 30.

- 1 K. S. Egorova and V. P. Ananikov, *Angew. Chem. Int. Ed.*, 2016, **55**, 12150–12162; *Angew. Chem.*, 2016, **128**, 12334–12347.
- 2 (a) I. Bauer and H.-J. Knölker, *Chem. Rev.*, 2015, **115**, 3170–3387; (b) A. Fürstner, *ACS Cent. Sci.*, 2016, **2**, 778–789; (c) R. Shang, L. Ilies and E. Nakamura, *Chem. Rev.*, 2017, **117**, 9086–9139; (d) S. Rana, J. P. Biswas, S. Paul, A. Paik and D. Maiti, *Chem. Soc. Rev.*, 2021, **50**, 243–472.



- 3 S. Rendic and F. P. Guengerich, *Chem. Res. Toxicol.*, 2015, **28**, 38–42.
- 4 C. Chapple, *Annu. Rev. Plant Physiol. Plant Mol. Biol.*, 1998, **49**, 311–343.
- 5 M. Mizutani and F. Sato, *Arch. Biochem. Biophys.*, 2011, **507**, 194–203.
- 6 R. J. Robins, N. C. J. E. Chesters, D. O'Hagan, A. J. Parr, N. J. Walton and J. G. Woolley, *J. Chem. Soc., Perkin Trans. 1*, 1995, 481–485.
- 7 K. Woithe, N. Geib, K. Zerbe, B. L. Dong, M. Heck, S. Fournier-Rousset, O. Meyer, F. Vitali, N. Matoba, K. Abou-Hadeed and J. A. Robinson, *J. Am. Chem. Soc.*, 2007, **129**, 6887–6895.
- 8 M. A. Bedewitz, A. D. Jones, J. C. D'Auria and C. S. Barry, *Nat. Commun.*, 2018, **9**, 5281.
- 9 N. Ikezawa, K. Iwasa and F. Sato, *J. Biol. Chem.*, 2008, **283**, 8810–8821.
- 10 P. F. X. Kraus and T. M. Kutchan, *Proc. Natl. Acad. Sci. U. S. A.*, 1995, **92**, 2071–2075.
- 11 F. P. Guengerich, *ACS Catal.*, 2018, **8**, 10964–10976.
- 12 (a) O. Augusto, H. S. Beilan and P. R. Ortiz De Montellano, *J. Biol. Chem.*, 1982, **257**, 11288–11295; (b) E. Baciocchi, O. Lanzalunga, A. Lapi and L. Manduchi, *J. Am. Chem. Soc.*, 1998, **120**, 5783–5787; (c) B. Chiavarino, R. Cipollini, M. E. Crestoni, S. Fornarini, F. Lanucara and A. Lapi, *J. Am. Chem. Soc.*, 2008, **130**, 3208–3217.
- 13 (a) C. Colombari, E. V. Kudrik, D. V. Tyurin, F. Albrieux, S. E. Nefedov, P. Afanasiev and A. B. Sorokin, *Dalton Trans.*, 2015, **44**, 2240–2251; (b) A. B. Sorokin, *Coord. Chem. Rev.*, 2019, **389**, 141–160.
- 14 M. S. Yusubov, C. Celik, M. R. Geraskina, A. Yoshimura, V. V. Zhdankin and V. N. Nemykin, *Tetrahedron Lett.*, 2014, **55**, 5687–5690.
- 15 R. Berger, G. Resnati, P. Metrangolo, E. Weber and J. Hulliger, *Chem. Soc. Rev.*, 2011, **40**, 3496–3508.
- 16 B. E. Smart, *J. Fluorine Chem.*, 2001, **109**, 3–11.
- 17 J. Leroy, A. Bondon, L. Toupet and C. Rolando, *Chem.–Eur. J.*, 1997, **3**, 1890–1893.
- 18 E. K. Woller and S. G. DiMagno, *J. Org. Chem.*, 1997, **62**, 1588–1593.
- 19 E. K. Woller, V. V. Smirnov and S. G. DiMagno, *J. Org. Chem.*, 1998, **63**, 5706–5707.
- 20 A. D. Adler, F. R. Longo, F. Kampas and J. Kim, *J. Inorg. Nucl. Chem.*, 1970, **32**, 2443–2445.
- 21 S. L. H. Rebelo, A. M. N. Silva, C. J. Medforth and C. Freire, *Molecules*, 2016, **21**, 481.
- 22 E. Tabor, J. Połowicz, K. Pamin, S. Basağ and W. Kubiak, *Polyhedron*, 2016, **119**, 342–349.
- 23 C. C. Guo, *J. Catal.*, 1998, **178**, 182–187.
- 24 A. Gold, K. Jayaraj, P. Doppelt, J. Fischer and R. Weiss, *Inorg. Chim. Acta*, 1988, **150**, 177–181.
- 25 ESI[†] for μ -oxo-bis[(octacosafuoro-meso-tetraphenylporphyrinato)iron(III)] (**5c**) have been deposited with the Cambridge Crystallographic Data Centre (CCDC 2209883).
- 26 A. B. Hoffman, D. M. Collins, V. W. Day, E. B. Fleischer, T. S. Srivastava and J. L. Hoard, *J. Am. Chem. Soc.*, 1972, **94**, 3620–3626.
- 27 L. P. Cailler, M. Clémancey, J. Barilone, P. Maldivi, J.-M. Latour and A. B. Sorokin, *Inorg. Chem.*, 2020, **59**, 1104–1116.
- 28 (a) E. Porhiel, A. Bondon and J. Leroy, *Tetrahedron Lett.*, 1998, **39**, 4829–4830; (b) S. Yokota, Y. Suzuki, S. Yanagisawa, T. Ogura, S. Nozawa, M. Hada and H. Fujii, *ACS Catal.*, 2022, **12**, 10857–10871.
- 29 (a) R. F. Fritsche, G. Theumer, O. Kataeva and H.-J. Knölker, *Angew. Chem. Int. Ed.*, 2017, **56**, 549–553; *Angew. Chem.*, 2017, **129**, 564–568; (b) A. Purtsas, O. Kataeva and H.-J. Knölker, *Chem.–Eur. J.*, 2020, **26**, 2499–2508; (c) A. Purtsas, S. Stipurin, O. Kataeva and H.-J. Knölker, *Molecules*, 2020, **25**, 1608; (d) A. Purtsas, M. Rosenkranz, E. Dmitrieva, O. Kataeva and H.-J. Knölker, *Chem.–Eur. J.*, 2022, **28**, e202104292.
- 30 R. F. Fritsche, T. Schuh, O. Kataeva and H.-J. Knölker, *Chem.–Eur. J.*, 2022, **28**, e202203269.
- 31 (a) C. Ercolani, G. Rossi and F. Monacelli, *Inorg. Chim. Acta*, 1980, **44**, L215–L216; (b) D.-H. Chin, G. N. La Mar and A. L. Balch, *J. Am. Soc. Chem.*, 1980, **102**, 4344–4350; (c) C. Ercolani, M. Gardini, K. S. Murray, G. Pennesi and G. Rossi, *Inorg. Chem.*, 1986, **25**, 3972–3976; (d) R. Dieing, G. Schmid, E. Witke, C. Feucht, M. Dreßen, J. Pohmer and M. Hanack, *Chem. Ber.*, 1995, **128**, 589–598.
- 32 (a) A. A. O. Sarhan and C. Bolm, *Chem. Soc. Rev.*, 2009, **38**, 2730–2744; (b) L. Zhai, R. Shukla, S. H. Wadumethrige and R. Rathore, *J. Org. Chem.*, 2010, **75**, 4748–4760; (c) M. Grzybowski, K. Skonieczny, H. Butenschön and D. T. Gryko, *Angew. Chem. Int. Ed.*, 2013, **52**, 9900–9930; *Angew. Chem.*, 2013, **125**, 10084–10115; (d) M. Grzybowski, B. Sadowski, H. Butenschön and D. T. Gryko, *Angew. Chem. Int. Ed.*, 2020, **59**, 2998–3027; *Angew. Chem.*, 2020, **132**, 3020–3050.
- 33 G.-Q. Chen, Z.-J. Xu, C.-Y. Zhou and C.-M. Che, *Chem. Commun.*, 2011, **47**, 10963–10965.
- 34 (a) T. Akiyama, J. Itoh, K. Yokota and K. Fuchibe, *Angew. Chem. Int. Ed.*, 2004, **43**, 1566–1568; *Angew. Chem.*, 2004, **116**, 1592–1594; (b) D. Uraguchi, K. Sorimachi and M. Terada, *J. Am. Chem. Soc.*, 2004, **126**, 11804–11805; (c) C. K. De, F. Pesciaoli and B. List, *Angew. Chem. Int. Ed.*, 2013, **52**, 9293–9295; *Angew. Chem.*, 2013, **125**, 9463–9465.
- 35 (a) H.-J. Knölker and K. R. Reddy, *Chem. Rev.*, 2002, **102**, 4303–4428; (b) H.-J. Knölker and K. R. Reddy in *The Alkaloids*, ed.: G. A. Cordell, Academic Press, Amsterdam, 2008, vol. 65, pp. 1–430; (c) I. Bauer and H.-J. Knölker, *Top. Curr. Chem.*, 2012, **309**, 203–253; (d) A. W. Schmidt, K. R. Reddy and H.-J. Knölker, *Chem. Rev.*, 2012, **112**, 3193–3328.
- 36 (a) G. Bringmann, S. Tasler, H. Endress, J. Kraus, K. Messer, M. Wohlfahrt and W. Lobin, *J. Am. Chem. Soc.*, 2001, **123**, 2703–2711; (b) P. N. M. Botman, M. Postma, J. Fraanje, K. Goubitz, H. Schenk, J. H. van Maarseveen and H. Hiemstra, *Eur. J. Org. Chem.*, 2002, 1952–1955; (c) J. L. Avila-Melo, A. Benavides, A. Fuentes-Gutiérrez, J. Tamariz and H. A. Jiménez-Vázquez, *Synthesis*, 2021, **53**, 2201–2211; (d) P. Sumsalee, L. Abella, T. Roisnel,



- S. Lebrequier, G. Pieters, J. Autschbach, J. Crassous and L. Favereau, *J. Mater. Chem. C*, 2021, **9**, 11905–11914.
- 37 C. Brütting, R. F. Fritsche, S. K. Kutz, C. Börger, A. W. Schmidt, O. Kataeva and H.-J. Knölker, *Chem.–Eur. J.*, 2018, **24**, 458–470.
- 38 (a) Isolation: P. Bhattacharyya, S. S. Jash and B. K. Chowdhury, *Chem. Ind.*, 1986, 246; (b) synthesis: R. Hesse, K. K. Gruner, O. Kataeva, A. W. Schmidt and H.-J. Knölker, *Chem.–Eur. J.*, 2013, **19**, 14098–14111.
- 39 (a) Isolation: T. Pacher, M. Bacher, O. Hofer and H. Greger, *Phytochemistry*, 2001, **58**, 129–135; synthesis: (b) K. K. Julich-Gruner, O. Kataeva, A. W. Schmidt and H.-J. Knölker, *Chem.–Eur. J.*, 2014, **20**, 8536–8540; (c) K. K. Julich-Gruner, A. W. Schmidt and H.-J. Knölker, *Synthesis*, 2014, **46**, 2651–2655.
- 40 (a) Isolation: C. Ito, Y. Thoyama, M. Omura, I. Kajiura and H. Furukawa, *Chem. Pharm. Bull.*, 1993, **41**, 2096–2100; previous syntheses: (b) H.-J. Knölker, H. Goesmann and C. Hofmann, *Synlett*, 1996, 737–740; (c) K. Dhara, T. Mandal, J. Das and J. Dash, *Angew. Chem. Int. Ed.*, 2015, **54**, 15831–15835; *Angew. Chem.*, 2015, **127**, 16057–16061; (d) ref. 37; (e) M. Sako, A. Sugizaki and S. Takizawa, *Bioorg. Med. Chem. Lett.*, 2018, **28**, 2751–2753.
- 41 (a) H.-J. Knölker, M. Bauermeister, D. Bläser, R. Boese and J.-B. Pannek, *Angew. Chem. Int. Ed.*, 1989, **28**, 223–225; *Angew. Chem.*, 1989, **101**, 225–227; (b) H.-J. Knölker, M. Bauermeister, J.-B. Pannek, D. Bläser and R. Boese, *Tetrahedron*, 1993, **49**, 841–862.
- 42 (a) Isolation: S. Karwehl, R. Jansen, V. Huch and M. Stadler, *J. Nat. Prod.*, 2016, **79**, 369–375; previous syntheses: (b) C. J. Moody and P. Shah, *J. Chem. Soc., Perkin Trans. 1*, 1989, 2463–2471; (c) M. Sako, K. Ichinose, S. Takizawa and H. Sasai, *Chem.–Asian J.*, 2017, **12**, 1305–1308; (d) M. Sako, S. Takizawa and H. Sasai, *Tetrahedron*, 2020, **76**, 131645.
- 43 ESI† for sorazolon E2 (**14c**) have been deposited with the Cambridge Crystallographic Data Centre (CCDC 2209872).
- 44 (a) R. Forke, M. P. Krahl, T. Krause, G. Schlechtingen and H.-J. Knölker, *Synlett*, 2007, 268–272; (b) R. Hesse, A. W. Schmidt and H.-J. Knölker, *Tetrahedron*, 2015, **71**, 3485–3490.
- 45 N.-K. Cao, Y.-M. Chen, S.-S. Zhu, K.-W. Zeng, M.-B. Zhao, J. Li, P.-F. Tu and Y. Jiang, *Phytochemistry*, 2020, **178**, 112463.
- 46 H. Sasabe, N. Toyota, H. Nakanishi, T. Ishizaka, Y.-J. Pu and J. Kido, *Adv. Mater.*, 2012, **24**, 3212–3217.
- 47 (a) Y. E. Kim, Y. S. Kwon, K. S. Lee, J. W. Park, H. J. Seo and T. W. Kim, *Mol. Cryst. Liq. Cryst.*, 2004, **424**, 153–158; (b) M. Reig, J. Puigdollers and D. Velasco, *J. Mater. Chem. C*, 2015, **3**, 506–513.
- 48 S. Mallick, S. Maddala, K. Kollimalayan and P. Venkatakrishnan, *J. Org. Chem.*, 2019, **84**, 73–93.
- 49 K. Matsumoto, Y. Toubaru, S. Tachikawa, A. Miki, K. Sakai, S. Koroki, T. Hirokane, M. Shindo and M. Yoshida, *J. Org. Chem.*, 2020, **85**, 15154–15166.
- 50 F. Puls and H.-J. Knölker, *Angew. Chem. Int. Ed.*, 2018, **57**, 1222–1226; *Angew. Chem.*, 2018, **130**, 1236–1240.
- 51 F. Puls, F. Seewald, V. Grinenko, H.-H. Klauß and H.-J. Knölker, *Chem.–Eur. J.*, 2021, **27**, 16776–16787.
- 52 F. Puls, O. Kataeva and H.-J. Knölker, *Eur. J. Org. Chem.*, 2018, 4272–4276.
- 53 F. Puls, P. Linke, O. Kataeva and H.-J. Knölker, *Angew. Chem. Int. Ed.*, 2021, **60**, 14083–14090; *Angew. Chem.*, 2021, **133**, 14202–14209.
- 54 (a) Isolation: T.-S. Wu, M.-L. Wang and P.-L. Wu, *Phytochemistry*, 1996, **43**, 785–789; previous syntheses: (b) D. P. Chakraborty and A. Islam, *J. Indian Chem. Soc.*, 1971, **48**, 91–92; (c) K. K. Gruner and H.-J. Knölker, *Org. Biomol. Chem.*, 2008, **6**, 3902–3904; (d) G. Chakraborti, S. Paladhi, T. Mandal and J. Dash, *J. Org. Chem.*, 2018, **83**, 7347–7359.
- 55 (a) M. C. Pangborn and R. J. Anderson, *J. Am. Chem. Soc.*, 1936, **58**, 10–14; (b) A. Ulubelen and T. Baytop, *Phytochemistry*, 1973, **12**, 1824; (c) J. O. Grimalt, L. Angulo, A. López-Galindo, M. C. Comas and J. Albaigés, *Chem. Geol.*, 1990, **82**, 341–363; (d) M. P. Rahelivao, T. Lübken, M. Gruner, O. Kataeva, R. Ralambondrahety, H. Andriamanantoanina, M. P. Checinski, I. Bauer and H.-J. Knölker, *Org. Biomol. Chem.*, 2017, **15**, 2593–2608.

